

# A new cell-sized support for 3D cell cultures based on recombinant spider silk fibers

Dganit Stern-Tal<sup>1</sup>, Shmulik Ittah<sup>2</sup> and Ella Sklan<sup>1</sup> 

Journal of Biomaterials Applications  
2022, Vol. 36(10) 1748–1757  
© The Author(s) 2021



Article reuse guidelines:  
[sagepub.com/journals-permissions](https://sagepub.com/journals-permissions)  
DOI: 10.1177/08853282211037781  
[journals.sagepub.com/home/jba](https://journals.sagepub.com/home/jba)



## Abstract

It is now generally accepted that 2D cultures cannot accurately replicate the rich environment and complex tissue architecture that exists *in vivo*, and that classically cultured cells tend to lose their original function. Growth of spheroids as opposed to 2D cultures on plastic has now been hailed as an efficient method to produce quantities of high-quality cells for cancer research, drug discovery, neuroscience, and regenerative medicine. We have developed a new recombinant protein that mimics dragline spidersilk and that self-assembles into cell-sized coils. These have high thermal and shelf-life stability and can be readily sterilized and stored for an extended period of time. The fibers are flexible, elastic, and biocompatible and can serve as cell-sized scaffold for the formation of 3D cell spheroids. As a proof of concept, recombinant spidersilk was integrated as a scaffold in spheroids of three cell types: primary rat hepatocytes, human mesenchymal stem cells, and mouse L929 cells. The scaffolds significantly reduced spheroid shrinkage and unlike scaffold-free spheroids, spheroids did not disintegrate over the course of long-term culture. Cells in recombinant spidersilk spheroids showed increased viability, and the cell lines continued to proliferate for longer than control cultures without spidersilk. The spidersilk also supported biological functions. Recombinant spidersilk primary hepatocyte spheroids exhibited 2.7-fold higher levels of adenosine triphosphate (ATP) continued to express and secrete albumin and exhibited significantly higher basal and induced CYP3A activity for at least 6 weeks in culture, while control spheroids without fibers stopped producing albumin after 27 days and CYP3A activity was barely detectable after 44 days. These results indicate that recombinant spidersilk can serve as a useful tool for long-term cell culture of 3D cell spheroids and specifically that primary hepatocytes can remain active in culture for an extended period of time which could be of great use in toxicology testing.

## Keywords

3D cell culture, scaffold, spheroids, spidersilk, hepatocytes, 3D model, drug screening model

## Introduction

During the last 15 years, it has become increasingly clear that monolayer cell cultures with cells attached to a polystyrene surface, or even to a surface coated with extracellular matrix compounds, do not completely reflect the conditions in the physiological 3D tissue. Cells on plastic dishes are polarized with their receptors concentrated on the surface in contact with the dish. They are also subjected to a number of differences, for example, with respect to permeation of oxygen, nutrients, or toxic compounds compared to the environment in the tissue. Without the native 3D network of interactions with extracellular matrix or with their neighbors, cells tend to de-differentiate.<sup>1-3</sup>

In consequence, monolayer cultures are often insufficient to provide a representative *in vitro* model, leading the researchers to perform the expensive *in vivo* studies, which themselves may also be insufficient, due to the differences between species.

Based on this need, multiple approaches have been developed to grow 3D cell cultures.<sup>4-10</sup>

One approach involves growing cells under conditions that minimize or avoid contact with the plastic surface, for example, in hanging drops. While avoiding the possibility of contact with the plastic surface, the cells tend to have contact with neighboring cells, forming 3D spheroids. However, in the absence of any biological matrix, the strong intracellular contacts lead to the eventual compaction of the spheroids<sup>11</sup> and cell death.<sup>12-16</sup>

<sup>1</sup>Seevix Material Sciences LTD, Jerusalem, Israel

<sup>2</sup>The Hebrew University of Jerusalem, Jerusalem, Israel

### Corresponding author:

Ella Sklan, Seevix Material Sciences LTD, Minrav Building, 4th floor, Hadassah Ein Kerem, Jerusalem 9112001, Israel.

Email: [ella@seevix.com](mailto:ella@seevix.com)

Another approach is preparing 3D scaffolds.<sup>7-9,17-20</sup> A wide variety of biological and artificial materials have been used to prepare macroscopic scaffolds, in order to allow cells to form 3D structures within a larger porous material. However, a major disadvantage is that the cells are not homogeneously distributed in the matrix<sup>21</sup> and in addition, problems in the diffusion of nutrients and oxygen may cause stagnation and have an adverse effect on cell viability and biological functions.<sup>9,22,23</sup>

The advantages of both approaches can be combined by using cell-sized scaffolds where the cells adhere to the porous matrix, thereby decreasing the tendency of the spheroid to shrink, while sustaining the 3D structure. In order to ensure an efficient supply of oxygen, the size of the spheroids including the scaffold should not be greater than a few hundred microns.<sup>4</sup>

One area that can particularly benefit from an improved method of 3D cell culture is preclinical toxicity testing.<sup>24</sup> In addition to the ethical desire to reduce the numbers of animal-based experiments, neither rodents nor 2D culture systems can recapitulate the human tumor microenvironment.<sup>25</sup> The alterations in growth conditions and interactions with surrounding cells or cell matrix frequently influence the response of the cells to drugs. These deficiencies probably contribute to the dismal rate of clinical success of drug development. There are similar difficulties in interpreting the preclinical results obtained with anti-cancer drugs.<sup>2</sup> Despite many attempts to prepare suitable cell lines, the gold standard for assessing drug-induced liver injury (DILI), a useful method for assessing drug toxicity, still employs primary hepatocytes. When seeded under conventional culture conditions, hepatocytes adhere to the plastic surface of the cell culture dish within 4 h and then aggregate in groups of 2–10 cells to re-establish intercellular contacts. Unfortunately, in classical 2D cultures, primary hepatocytes start to lose activity after only a few days,<sup>26-28</sup> making them applicable only for acute toxicity studies. The solution appears to be hepatocyte spheroids, which have been reported to live longer in culture and maintain function in that they continue to secrete albumin and can be stimulated to express the cytochrome P450 (CYP) genes that are required for detoxification of applied materials.<sup>1,27-31</sup> Such spheroids made of cryopreserved hepatocytes were reported to be phenotypically and functionally stable for 2–3 weeks, and in case of freshly produced hepatocytes for even up to 5 weeks in culture, and to maintain endogenous hepatic functions, such as albumin and urea production as well as glycogen storage.<sup>27,29,32</sup> Naturally produced spheroids are useful but are soft and somewhat difficult to manipulate. In the absence of any biological matrix, the strong intracellular contacts may lead to the eventual compaction of the spheroids<sup>11</sup> and cell death.<sup>28,33</sup> Natural spidersilk is a material that combines a toughness comparable to that of steel, with elasticity and versatility.<sup>34-36</sup> In addition, it is

extensible and well tolerated by biological systems. Substrates prepared from natural spidersilk<sup>37-39</sup> or recombinant spidersilk-based proteins<sup>40-46</sup> have been shown to facilitate the adherence of cultured cells and support growth of material for tissue engineering.<sup>47-49</sup>

We have developed a new material, composed of cell-sized coils of fibers made from a recombinant dragline spidersilk protein. The artificial sequence is based on the sequence of *Araneus diadematus* spidersilk dragline ADF4 protein. The fibers are produced in insect cells, using a baculovirus expression system. Our unique process of self-assembly of fibers inside the cells generates fibers (SpheroSeev) with structural characteristics similar to those of the natural dragline.<sup>50,51</sup>

The final fibers are highly water-insoluble and can withstand temperatures up to 235°C, allowing them to be sterilized by autoclave incubation. A single recombinant spidersilk fiber coil has a diameter of about 15 µm, which is comparable to the size of a single cell. This makes the fibers very suitable for use as a scaffold for the preparation of cell spheroids. Cells grown in the presence of our spidersilk form spheroids. As proof of concept, we present here the effects of recombinant spidersilk fibers on the formation of cell spheroids, cell viability within the spheroids, and the biological functions of cultured cells. Efficient cellular growth with an extended period of survival and function were seen in three cell types tested: primary rat hepatocytes, human mesenchymal stem cells (hMSC), and mouse L929 cells.

## Materials and methods

### Preparation of spidersilk fibers

Recombinant Spidersilk fibers (SpheroSeev) were produced by Seevix Material Sciences Ltd. and expressed in insect cells<sup>50,51</sup> by a proprietary procedure. To stain spidersilk coils with anti-His-tag antibodies, the insect cells were fixed with methanol, permeabilized, and stained with monoclonal anti-His-tag antibody (MBL international). After washing, they were stained with Alexa 594-labeled goat anti-mouse antibody (Jackson Laboratories).

### Cells and cell culture conditions

NCTC clone 929 (L929) cells (ATCC CCL-1) and adipose-derived mesenchymal stem cells (MSC) (hMSC, ATCC PCS-500-011) were purchased from the ATCC. Primary rat hepatocytes were obtained from Kurabo Industries, Japan.

L929 were cultured in MEM-NEAA medium supplemented with 10% horse serum, 2 mM L-glutamine, and 1 mM sodium pyruvate. The hMSCs were cultured in MSC

Basal Medium (ATCC PSC-500-030) supplemented with MSC Growth Kit and 100 U/ml penicillin-0.1 mg/mL, streptomycin-0.25  $\mu$ g/ml, and amphotericin B (Biological industries). Rat primary hepatocytes were cultured in Williams E medium (Sigma) supplemented with 10% inactivated FBS (Biological industries), 2 mM L-glutamine (Sigma), 1.72  $\mu$ M insulin (Lifetech), 0.07  $\mu$ M transferrin (Lifetech), 0.04  $\mu$ M selenium (Lifetech), and 0.1  $\mu$ M dexamethasone (Sigma).

### Preparation of spheroids

The procedure for preparing the spheroids is summarized in Figure 1. Briefly, primary rat hepatocyte cells were thawed according to the manufacturer's instructions. L929 cells and hMSCs were dissociated with trypsin-EDTA (Biological Industries), then were neutralized, and counted with trypan blue to assess viability. Seeding stock was prepared by diluting the cells in growth media (control group) or media containing different concentrations of spidersilk. The

samples were dispensed into ultra-low attachment (ULA) plates (Nunc/Sphera, NUNC) and incubated at 37°C, 5% CO<sub>2</sub> to allow spheroids to form. Every 2 days (hepatocytes), or 4 days (cell lines), half the medium in each well was replaced with fresh medium. For albumin measurements, supernatants collected from hepatocyte cultures were stored at -20°C.

### Staining with PI and PI/calcein

To assess cell viability and spheroid morphology, control and treated spheroids were collected into a 1.5 mL tube, washed twice in PBS (Biological Industries) by allowing the tube to stand for 2 min until spheroids sink, aspirating the medium, and replacing with 0.5 mL fresh PBS. Spheroids were stained with 2  $\mu$ M calcein-AM (Cayman Chemical) and 50  $\mu$ g/ml propidium iodide (Sigma) diluted in PBS. Spheroids were incubated with the dyes for 15 min and then images were collected with a FV-1200 confocal microscope, Olympus, Japan. Images were analyzed by ImageJ software.

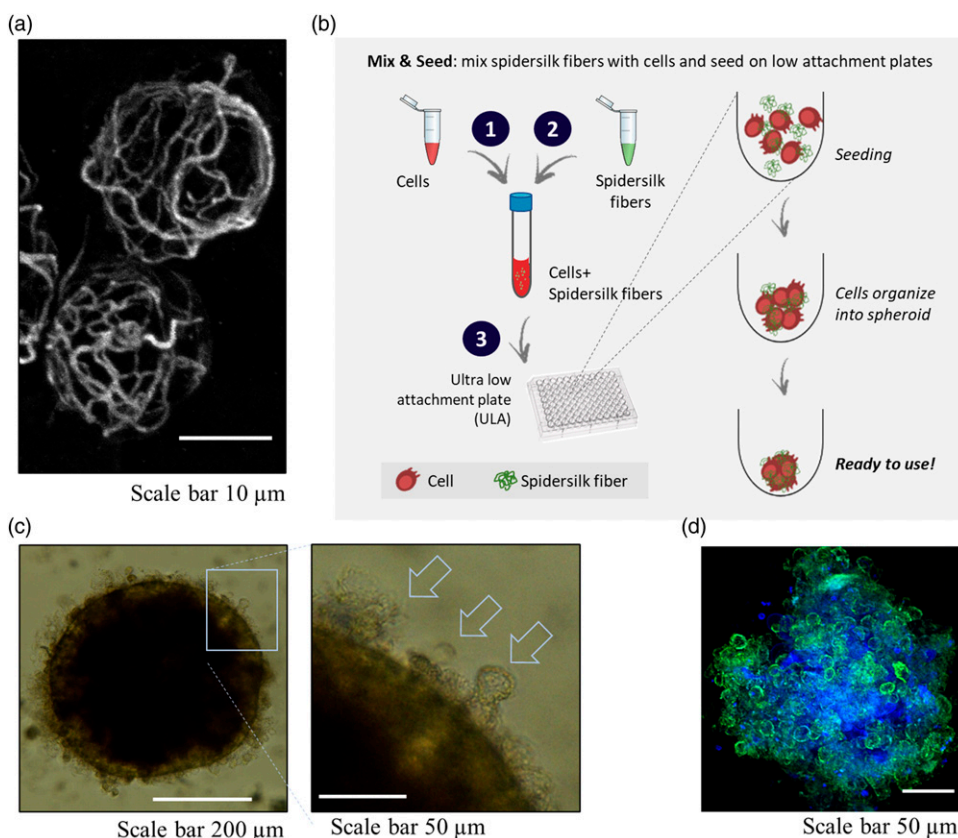


**Figure 1.** (a) Typical recombinant spidersilk coils within the insect cells during production process. Staining with mouse monoclonal anti-His-tag antibody and Alexa 594 goat anti-mouse IgG. (b) Spheroid assembly: fibers and cells are mixed and seeded on an ultra-low attachment plate. Over the following days, the cells form aggregates containing trapped fibers and eventually establish cell-cell interactions to make stable spheroids. (c) Spheroid composed of primary rat hepatocytes at day 27 of culture. Recombinant spidersilk fibers integrated into the spheroids can be observed on the margins of the spheroid (indicated by the arrows). (d) Mesenchymal stem cell spheroids stained with thioflavin S: green- beta sheets containing fibers; blue- non-specific staining of cells.

### Staining with thioflavin S

Thioflavin S (Merck) is a fluorescent stain that changes the excitation and emission spectra when bound to beta sheet rich structures to give a green color.

For thioflavin S staining, spheroids were incubated in PBS supplemented with 25  $\mu$ M thioflavin S (Merck) for 15 min. Spheroids were washed in PBS and then images were collected with a FV-1200 confocal microscope, Olympus, Japan.

### Measurement of ATP

Viability and proliferation of the cells were measured using a CellTiter-Glo 3D Cell Viability Assay (Promega) based on quantitation of the cellular ATP levels, according to the manufacturer's instructions for use.

### Measurement of albumin

Albumin levels were measured in the supernatant collected from hepatocytes by using a rat albumin ELISA quantitation set (Bethyl laboratories) according to the manufacturer's instructions.

### Measurement of CYP3A activity

CYP3A activity was measured using a P450-Glo™ CYP3A4 assay kit (Promega) according to the manufacturer's instructions for use. For CYP3A induction, spheroids were exposed to 50  $\mu$ M dexamethasone (Sigma) for 48 h before measurement.

### Statistics

The experimental groups were compared with the controls using unpaired two-tailed *t*-test. The *p* values are presented for each quantitative experiment. A *p* value below 0.05 was considered statistically significant.

## Results

### Preparation of Spidersilk fibers

Spidersilk fibers were prepared using recombinant DNA technology. A protein biomimicking dragline spidersilk protein was expressed in insect cells and self-assembled inside the cells into coils. [Figure 1\(a\)](#) shows the formation of the spidersilk coils in the insect cells.

When spidersilk coils were incubated with different types of cells in ULA plates according to the scheme showed in [Figure 1\(b\)](#), the cells formed aggregates containing trapped fibers and eventually established cell–cell interactions to make stable spheroids with the fibers

integrated into the structure ([Figure 1\(c\)](#)). Spidersilk fibers intercalated into spheroids were stained with thioflavin S, a fluorescent dye that changes its excitation and emission spectra when bound to beta sheet rich structures. Spidersilk fibers are rich in beta sheets and therefore fluorescent green when bound to thioflavin S. In contrast, non-specific binding of thioflavin S appears blue. The green fluorescence shown in [Figure 1\(d\)](#) indicates that the spidersilk fibers are present throughout the spheroid and maintain the beta sheet conformation.

### Effect of spidersilk on spheroid size, integrity, and viability

Primary rat hepatocytes formed spheroids in the non-adhesive plates even without the addition of spidersilk coils. However, in the presence of spidersilk coils, even after the first day of culture, hepatocytes seeded at 7500 cells with 0.4 ng/cell spidersilk formed spheroids that were 18.5% larger than those without added coils ( $p < 0.001$ , unpaired *t*-test, [Figure 2\(a\)](#)).

Spidersilk fiber-free spheroids compacted during culture, and by day 17, their size had decreased to 44% of the start diameter (the size on day 1 of culture). This percentage decrease was similar over a seeding range of 1500–7500 cells/well (data not shown). However, in the presence of spidersilk fibers, the shrinkage was moderated, and on day 17 of culture, the spheroids grown in the presence of spidersilk had lost only 35% of their diameter and were 78% larger than the spidersilk-free controls ( $p < 0.001$ , unpaired *t*-test, [Figure 2\(b\)](#)).

In contrast to the non-proliferating primary hepatocytes, L929 fibroblasts and hMSCs can proliferate in culture under appropriate conditions. L929 spheroids seeded at 5000 cells/well grew in size even without spidersilk ([Figure 2\(c\)](#)). However, in the presence of 0.4 ng spidersilk/cell, the diameter of the spheroids increased still more indicating higher proliferation for a longer period. By day 8, the diameter of spidersilk L929 spheroids was 56% higher than that of spidersilk-free spheroids ( $p < 0.001$ , unpaired *t*-test). In contrast, spheroids formed from hMSCs seeded at 1500 cells/well did not increase in size but did grow in a dose-dependent manner when spidersilk coils were added ([Figure 2\(d\)](#)). By day 14, the diameter of spheroids seeded with 0.6 and 2 ng spidersilk/cell were 3.1- and 5.1-fold, respectively, greater than control spheroids ( $p < 0.001$ , unpaired *t*-test). These spheroids maintained their size for at least 18 more days in culture.

The ability of the spidersilk to increase the stability of the cells over long-term culturing is demonstrated in [Figure 3\(a\)](#). Cryopreserved primary hepatocytes cultured without spidersilk spontaneously formed spheroids that disintegrated into single cells by day 37 of culture, while in



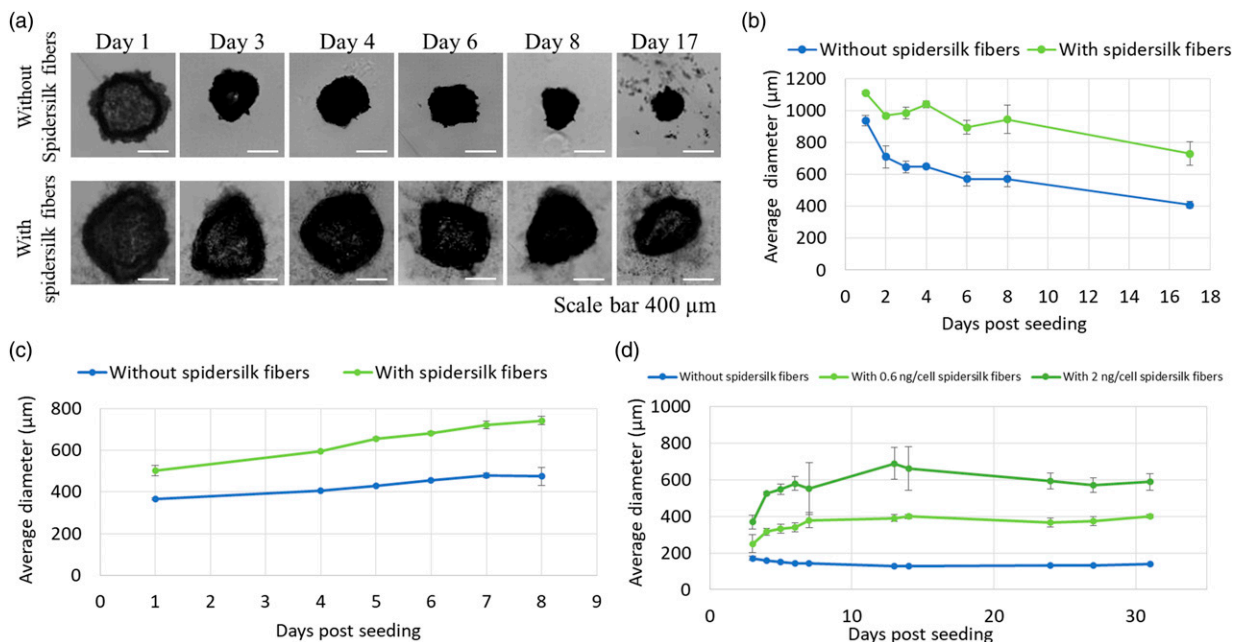


**Figure 2.** Effects of spidersilk on spheroid size and integrity of primary rat hepatocytes, MSCs, and L929 cells. (a) Primary rat hepatocytes seeded with and without spidersilk fibers (0.4 ng/cell) and cultured at 7500 cells/well, as described in “Materials and Methods.” Spheroids were imaged at the indicated time points with a light microscope, and their size was measured with ImageJ software (NIH). (b) The average spheroid diameter of non-proliferating hepatocytes (7500 cells seeded/well seeded with or without 0.4 ng spidersilk/cell). Data points represent the mean spheroid diameter ± SD (for each point, N = 4). (c) Proliferating L929 cells (5000 cells seeded with or without 0.4 ng/cell spidersilk) and (d) MSCs (1500 cells seeded with or without 0.2–0.4 ng recombinant spidersilk/cell). Data points represent the mean spheroid diameter ± SD (for each point, N = 3). MSC: mesenchymal stem cell.

the presence of spidersilk coils, the spheroids remained intact. Staining the spheroids with calcein AM (live cells stain green) and PI (dead cells stain red) indicated that the cells in the spheroids grown with spidersilk appeared green and were therefore viable, while not only were the spheroids smaller without spidersilk, but the cells were already dying after 7 days in culture (presence of red staining, Figure 3(b)). The L929 spheroids were seeded at 5000 cells/well, which generates large spheroids. At days 5 and 7, those grown in the presence of spidersilk coils (Figure 3(c)) were large and not necessarily round. In contrast, the corresponding spheroids without spidersilk were much smaller and classically spherical. On day 5, the spheroids without spidersilk already contained a prominent core of dead cells in the center of the spheroid; while in the presence of spidersilk, there were only individual dead cells dispersed throughout the spheroid. By day 7, a central core of dead cells had also appeared in the spidersilk spheroids but still occupied a smaller percentage of the whole spheroid than those grown in the absence of fibers.

Human mesenchymal stem cell spheroids in the absence of spidersilk looked shrunken (Figure 3(d)), with a significant number of dead cells (as shown by PI staining). In contrast, spheroids in the presence of spidersilk (4 ng/cell)

were much larger, with very few dead cells. In addition, the morphology of cells in the spidersilk spheroids was more spread, whereas cells in the spidersilk-free spheroids appeared rounder, which is known to influence the fate of MSCs in the culture.

The intracellular ATP concentration is also a measure of cellular viability and activity. Assays of primary rat hepatocytes spheroids cultured for 18 days revealed that the presence of spidersilk increased the levels of ATP in the spheroids (i.e., number of metabolically active cells) by 68% ( $p < 0.001$ , unpaired  $t$ -test). On day 44, the level of ATP was 2.7-fold higher in cells cultured with spidersilk ( $p < 0.05$ , unpaired  $t$ -test) (Figure 4(a)). This indicates that the cells grown with the spidersilk remain viable and active for at least 6 weeks in culture, which represents a significant advance over regular cultures of primary hepatocytes.

The addition of spidersilk also improved the intracellular ATP concentration of L929 spheroids, which increased by 37% on day 4 ( $p < 0.05$ , unpaired  $t$ -test), and by 62% at day 6 of culture compared to control cultures without fibers ( $p < 0.05$ , unpaired  $t$ -test, Figure 4(b)). The viability of hMSCs spheroids seeded without spidersilk decreased slowly but continuously throughout the experiment. In contrast, spidersilk-containing spheroids continued to proliferate for 24 days and maintained high viability for at least 30 days

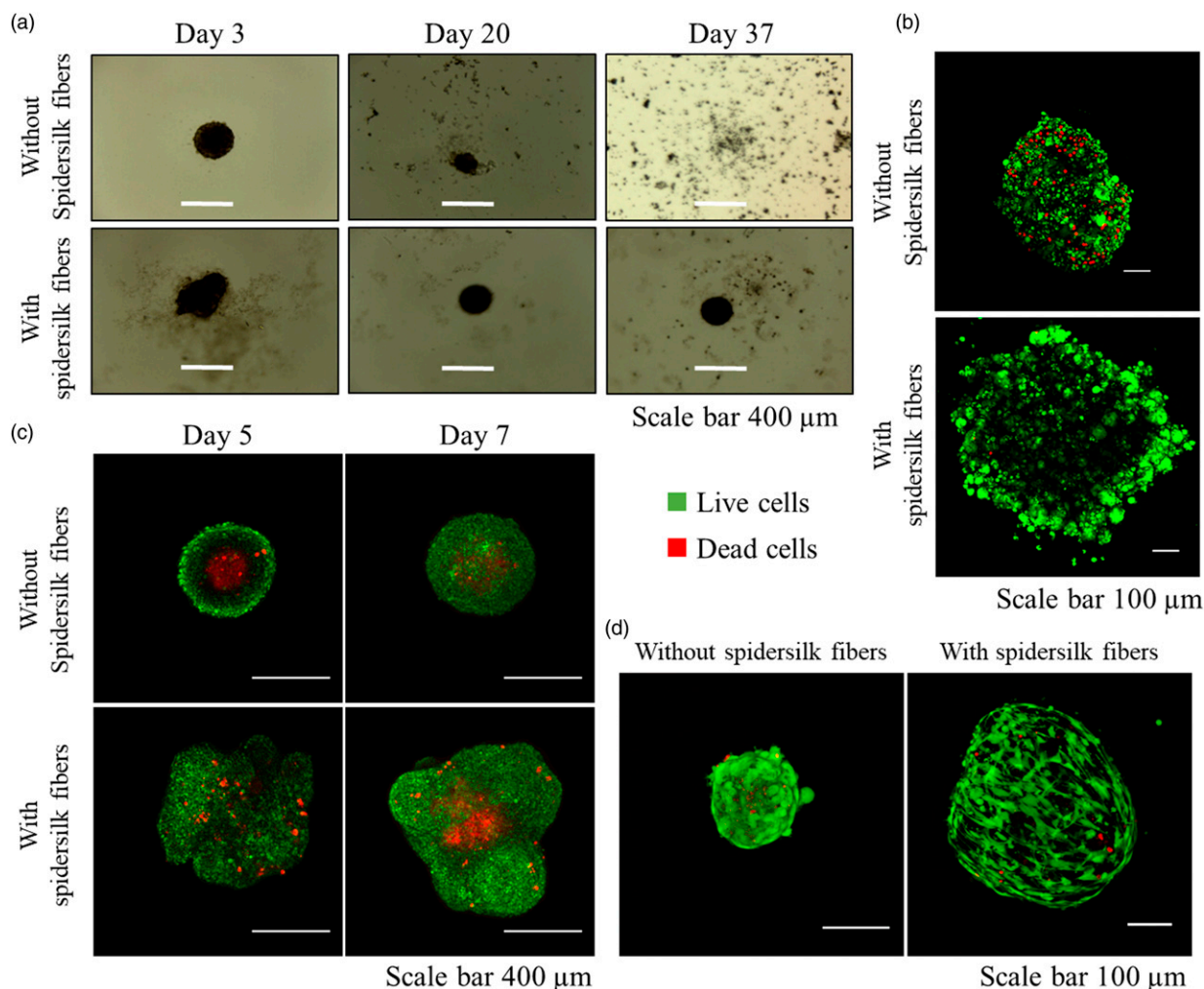


**Figure 3.** Effect of recombinant spidersilk on spheroid morphology, integrity, and cellular viability (a) Primary rat hepatocytes seeded with and without recombinant spidersilk fibers (0.4 ng/cell) and cultured at 1500 cells/well. Spheroids were imaged with a light microscope at the indicated days to assess their integrity. The morphology and viability of (b) primary hepatocyte spheroids (day 7 of culture, 5000 cells seeded/well), (c) L929 cells (day 5 and day 7 of culture, 5000 cells seeded/well), and (d) mesenchymal stem cells (day 7 of culture, 1000, cells seeded/well, 2 ng spidersilk/cell) were evaluated by fluorescent staining of the cells. The live cells are stained with calcein AM (green), the dead cells—with PI (red). The bar corresponds to 100  $\mu\text{m}$ .

(Figure 4(c)). Seeding MSC spheroids with 2 ng spidersilk/cell resulted in higher viability than seeding with 0.6 ng spidersilk/cell. At days 24–30, although the spheroids did not increase in size, the viability of cells grown with 2 ng/cell spidersilk was 7–8-fold higher than those grown without spidersilk ( $p < 0.01$ , unpaired  $t$ -test).

#### Biological function of rat hepatocytes

The functionality of hepatocytes can be monitored by the ability to secrete serum proteins, specifically albumin, and by the enzymatic activity of CYP3A, a member of the cytochrome P450 superfamily, the major enzymes involved in drug metabolism.

#### Albumin secretion

The ability of cultured rat hepatocytes to produce albumin was increased by inclusion of spidersilk fibers (Figure 5(a)). At day 14 of culture, albumin secretion by hepatocytes in spidersilk spheroids was 96% higher than in control spheroids and continued for many days after cells grown without spidersilk had essentially ceased to secrete any detectable albumin at all. Albumin production by cells grown with spidersilk was still easily quantifiable up to day 44. The results demonstrate that spidersilk both increased the maximal expression and prolonged the period of expression. The effect was particularly prominent at low cell concentrations.

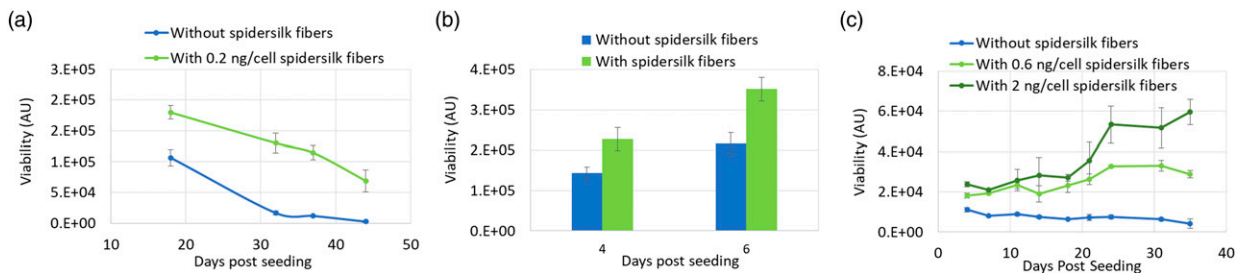


**Figure 4.** Effect of recombinant spidersilk fibers on spheroid cell viability/proliferation. (a) Long-term viability of rat primary hepatocytes seeded at 1500 cells/well with 0.2 ng/cell spidersilk, or without spidersilk, was evaluated by ATP quantification at the indicated time points. Each point represents the average of three replicates  $\pm$  SD. Proliferation rates of (b) L929 cells seeded at 2500 cells/well and (c) mesenchymal stem cells seeded at 1500 cells/well were evaluated by ATP quantification at the indicated time points. Each point represents the average of three replicates  $\pm$  SD.

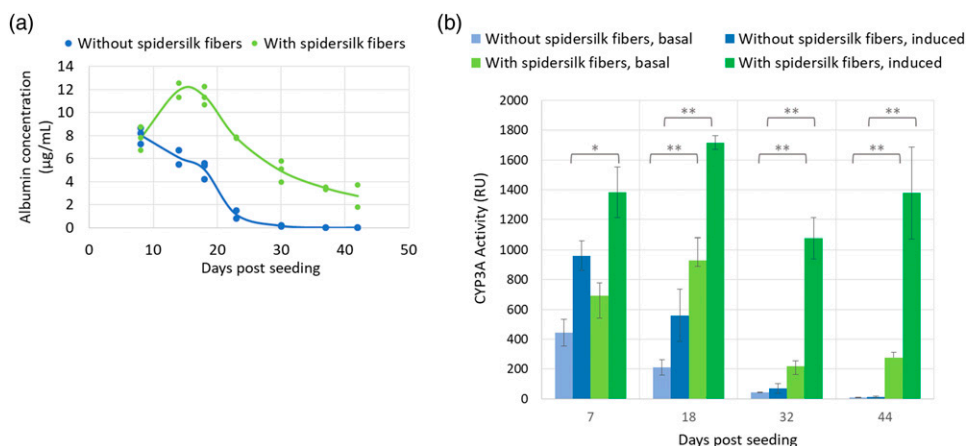


**Figure 5.** Recombinant spidersilk fibers support the function of spheroid hepatocytic nature for a longer period of time. (a) Effect of recombinant spidersilk (0.2 ng/cell) on albumin secretion by rat primary hepatocytes (1500 cells/well). Each data point represents a single measurement. For each time point, 2–3 measurements are presented. (b) Effect of recombinant spidersilk (0.2 ng/cell) on basal and dexamethasone-induced CYP3A activity (1500 cells/well). The data points represent mean  $\pm$  SD. (\*:  $p < 0.02$ , \*\*:  $p < 0.003$ , unpaired  $t$ -test).

### CYP3A activity

Functionality of primary hepatocyte spheroids cultured with and without spidersilk coils was assessed by CYP3A activity measurement. In addition to the basal CYP3A activity, cells were also treated with dexamethasone, to induce CYP3A as described previously.<sup>52</sup> As shown in Figure 5(b), both basal and induced CYP3A activity were higher in spheroids cultured with spidersilk fibers. After 18 days in culture, basal and induced CYP3A activity was 4.6- and 3-fold higher (respectively) in spheroids generated with spidersilk compared to those without (basal CYP3A  $p < 0.001$ , induced CYP3A  $p < 0.05$ , unpaired  $t$ -test). At day 32, basal and induced CYP3A activity was 5- and 16-fold higher (respectively) in spheroids generated with spidersilk (basal CYP3A  $p = 0.001$ , induced CYP3A  $p < 0.001$ , unpaired  $t$ -test). Notably, after 44 days of culture, CYP3A activity was barely detectable in control spheroids while still easily measured in spidersilk spheroids, reaching a 30-fold

higher basal activity and 109-fold higher induced activity (basal CYP3A  $p < 0.001$ , induced CYP3A  $p < 0.005$ , unpaired  $t$ -test). This indicates that even after extended culture, the hepatocytes grown with spidersilk remained active and suitable for use in toxicity assays.

### Discussion

We have produced recombinant spidersilk fibers that are made of a stable, elastic, and versatile natural compound and serve as cell-sized scaffolds. The use of the recombinant spidersilk may combine the advantages of two approaches used in 3D cultures, by reducing undesirable spheroid shrinkage and cell death without the formation of a large-scale supporting matrix that prevents free penetration of chemicals and oxygen. Since the scaffold is comprised of discrete particles, it is homogeneously distributed throughout the spheroid.

Cultures of all the cell types described here grew better in the presence of the spidersilk coils. This was reflected in a higher viability and activity (ATP assay) in culture over a longer period of time and improved proliferation of dividing cells (fibroblasts and MSCs). We have a particular interest in the primary hepatocyte cultures, in which albumin production and CYP3A activity remained high for over 6 weeks in culture; cells after 44 days in culture with the spidersilk coils responded to induction with dexamethasone over 100-fold better than cultures of primary hepatocytes cultured without the spidersilk coils. This could be of great use in drug toxicity screening, by extending the time frame available for testing DILI. Significantly, 27% of the drugs withdrawn due to toxicity between 1990–2010 were due to DILI,<sup>53</sup> which reflects the failure of animal models to recapitulate human metabolism. The increase in the time window could make it possible to conduct repeat tests and longer-term studies, which are very desirable in this context.<sup>29</sup>

In this study, we emphasized the properties of this unique scaffold in the context of spheroids; however, we believe that future applications for recombinant spidersilk fibers will extend far beyond this phenomenon. Significantly, spidersilk is known to be biocompatible and is well tolerated when implanted.<sup>43,54,55</sup>

Recently, in accordance with our results, microfibers hydrolyzed from silkworm and incorporated into bone marrow stem cell spheroids were shown to promote higher cell viability and osteogenic differentiation.<sup>56</sup>

The results presented here show that naturally folded and spontaneously self-assembled recombinant spidersilk can provide a distinctive structure and architecture, with exceptional flexibility and a vast surface area. We believe that the effects of the recombinant spidersilk fibers on spheroid viability and functionality are related to the dimensions, structure, and mechanical properties of the fibers. The structure, composed of nano-dimension fibrils intertwined to form micro-dimension coils, supports the cells in an ECM-like manner, providing a tissue-like environment. The high porosity of the coils permits better penetration of oxygen, nutrients, and waste removal enabling the culture of larger spheroids, not limited to 100–200  $\mu\text{m}$ . The combination of dimensions, unique mechanical properties of the fibers, and the ability to spontaneously adhere to cells give them the capacity to create a personal scaffold for individual cells.

### Acknowledgments

We would like to thank Kurabo Industries, Japan, for providing the primary rat hepatocytes. We are grateful to Naomi Melamed-Book for performing the confocal microscopy.

### Declaration of conflicting interests

The author(s) declared no potential conflicts of interest with respect to the research, authorship, and/or publication of this article.

### Funding

The author(s) received no financial support for the research, authorship, and/or publication of this article.

### ORCID iD

Ella Sklan  <https://orcid.org/0000-0002-0369-4648>

### References

1. Fraczek J, Bolleyn J, Vanhaecke T, et al. Primary hepatocyte cultures for pharmaco-toxicological studies: at the busy crossroad of various anti-dedifferentiation strategies. *Arch Toxicol* 2013; 87: 577–610.
2. Costard LS, Hosn RR, Ramanayake H, et al. Influences of the 3D microenvironment on cancer cell behaviour and treatment responsiveness: a recent update on lung, breast and prostate cancer models. *Acta Biomaterialia* 2021; Available online. In press.
3. Jensen C and Teng Y. Is it time to start transitioning from 2D to 3D cell culture?. *Frontiers in Molecular Biosciences* 2020; 7: 33.
4. Laschke MW and Menger MD. Life is 3D: boosting spheroid function for tissue engineering. *Trends in Biotechnology* 2017; 35: 133–144.
5. Antoni D, Burckel H, Josset E, et al. Three-dimensional cell culture: a breakthrough in vivo. *International Journal of Molecular Sciences* 2015; 16: 5517–5527.
6. Bates R, Edwards NS and Yates JD. Spheroids and cell survival. *Critical Reviews in Oncology/Hematology* 2000; 36: 61–74.
7. Fitzgerald KA, Malhotra M, Curtin CM, et al. Life in 3D is never flat: 3D models to optimise drug delivery. *Journal of Controlled Release: Official Journal of the Controlled Release Society* 2015; 215: 39–54.
8. Ravi M, Paramesh V, Kaviya SR, et al. 3D cell culture systems: advantages and applications. *Journal of Cellular Physiol* 2015; 230: 16–26.
9. Knight E and Przyborski S. Advances in 3D cell culture technologies enabling tissue-like structures to be created in vitro. *Journal of Anatomy* 2015; 227: 746–756.
10. Park Y, Huh KM and Kang S-W. Applications of biomaterials in 3D cell culture and contributions of 3D cell culture to drug development and basic biomedical research. *International Journal of Molecular Sciences* 2021; 22(5): 2491.
11. Lin RZ, Chou LF, Chien CCM, et al. Dynamic analysis of hepatoma spheroid formation: roles of E-cadherin and beta1-integrin. *Cell and Tissue Research* 2006; 324: 411–422.
12. Luebke-Wheeler JL, Nedredal G, Yee L, et al. E-cadherin protects primary hepatocyte spheroids from cell death by a caspase-independent mechanism. *Cell transplantation* 2009; 18: 1281–1287.
13. Bell HS, Whittle IR, Walker M, et al. The development of necrosis and apoptosis in glioma: experimental findings using spheroid culture systems. *Neuropathol and applied neurobiology* 2001; 27: 291–304.



14. Tong JZ, De Lagausic P, Furlan V, et al. Long-term culture of adult rat hepatocyte spheroids. *Experimental Cell Research* 1992; 200: 326–332.
15. Anada T, Fukuda J, Sai Y, et al. An oxygen-permeable spheroid culture system for the prevention of central hypoxia and necrosis of spheroids. *Biomaterials* 2012; 33: 8430–8441.
16. Glicklis R, Merchuk JC and Cohen S. Modeling mass transfer in hepatocyte spheroids via cell viability, spheroid size, and hepatocellular functions. *Biotechnol and Bioengineering* 2004; 86: 672–680.
17. Tibbitt MW and Anseth KS. Hydrogels as extracellular matrix mimics for 3D cell culture. *Biotechnol and Bioengineering* 2009; 103: 655–663.
18. Carletti E, Motta A and Migliaresi C. Scaffolds for tissue engineering and 3D cell culture. *Methods in Molecular Biology (Clifton, NJ)* 2011; 695: 17–39.
19. Dutta RC and Dutta AK. Cell-interactive 3D-scaffold; advances and applications. *Biotechnol Advances* 2009; 27: 334–339.
20. Hogrebe NJ, Reinhardt JW and Gooch KJ. Biomaterial microarchitecture: a potent regulator of individual cell behavior and multicellular organization. *Journal of Biomedical Materials Research Part A* 2017; 105: 640–661.
21. Baptista LS, Kronemberger GS, Côrtes I, et al. Adult stem cells spheroids to optimize cell colonization in scaffolds for cartilage and bone tissue engineering. *International Journal of Molecular Sciences* 2018; 19(5): 1285.
22. Verjans ET, Doijen J, Luyten W, et al. Three-dimensional cell culture models for anticancer drug screening: worth the effort? *Journal of Cellular Physiol* 2018; 233: 2993–3003.
23. Jongpaiboonkit L, King WJ, Lyons GE, et al. An adaptable hydrogel array format for 3-dimensional cell culture and analysis. *Biomaterials* 2008; 29: 3346–3356.
24. Hughes DJ, Kostrzewski T and Sceats EL. Opportunities and challenges in the wider adoption of liver and interconnected microphysiological systems. *Experimental biology and medicine (Maywood, NJ)* 2017; 242: 1593–1604.
25. Pinto B, Henriques AC, Silva PMA, et al. Three-dimensional spheroids as in vitro preclinical models for cancer research. *Pharmaceutics* 2020; 12(12): 1186.
26. Ruoß M, Vosough M, Königsrainer A, et al. Towards improved hepatocyte cultures: progress and limitations. *Food and Chemical Toxicology* 2020; 138: 111188.
27. Mizoi K, Arakawa H, Yano K, et al. Utility of three-dimensional cultures of primary human hepatocytes (spheroids) as pharmacokinetic models. *Biomedicines* 2020; 8(10): 374.
28. Godoy P, Hewitt NJ, Albrecht U, et al. Recent advances in 2D and 3D in vitro systems using primary hepatocytes, alternative hepatocyte sources and non-parenchymal liver cells and their use in investigating mechanisms of hepatotoxicity, cell signaling and ADME. *Arch Toxicol* 2013; 87: 1315–1530.
29. Bell CC, Dankers ACA, Lauschke VM, et al. Comparison of hepatic 2D sandwich cultures and 3D spheroids for long-term toxicity applications: a multicenter study. *Toxicol Sci* 2018; 162: 655–666.
30. Gómez-Lechón MJ, Tolosa L, Conde I, et al. Competency of different cell models to predict human hepatotoxic drugs. *Expert Opin Drug Metab Toxicol* 2014; 10: 1553–1568.
31. den Braver-Sewradj SP, den Braver MW, Vermeulen NPE, et al. Inter-donor variability of phase I/phase II metabolism of three reference drugs in cryopreserved primary human hepatocytes in suspension and monolayer. *Toxicol In Vitro* 2016; 33: 71–79.
32. Bell CC, Hendriks DFG, Moro SML, et al. Characterization of primary human hepatocyte spheroids as a model system for drug-induced liver injury, liver function and disease. *Scientific reports* 2016; 6: 25187.
33. Białkowska K, Komorowski P, Bryszewska M, et al. Spheroids as a type of three-dimensional cell cultures-examples of methods of preparation and the most important application. *International Journal of Molecular Sciences* 2020; 21: 6225.
34. Humenik M, Scheibel T and Smith A. Spider silk: understanding the structure-function relationship of a natural fiber. *Prog Mol Biol Transl Sci* 2011; 103: 131–185.
35. Harmer AMT, Blackledge TA, Madin JS, et al. High-performance spider webs: integrating biomechanics, ecology and behaviour. *J R Soc Interface* 2011; 8: 457–471.
36. Belbéoch C, Lejeune J, Vroman P, et al. Silkworm and spider silk electrospinning: a review. *Environmental Chemistry Letters* 2021; 19(2): 1737–1763.
37. Hafner K, Montag D, Maeser H, et al. Evaluating adhesion and alignment of dental pulp stem cells to a spider silk substrate for tissue engineering applications. *Mater Sci Eng C Mater Biol Appl* 2017; 81: 104–112.
38. Kuhbier JAW, Alleging C, Reamers K, et al. Interactions between spider silk and cells—NIH/AT fibroblasts seeded on miniature weaving frames. *Plovs One* 2010; 5: e12032.
39. Hakimi O, Gheysens T, Vollrath F, et al. Modulation of cell growth on exposure to silkworm and spider silk fibers. *Journal of biomedical materials research Part A* 2010; 92: 1366–1372.
40. Widhe M, Bysell H, Nystedt S, et al. Recombinant spider silk as matrices for cell culture. *Biomaterials* 2010; 31: 9575–9585.
41. Wendt H, Hillmer A, Reamers K, et al. Artificial skin—culturing of different skin cell lines for generating an artificial skin substitute on cross-woven spider silk fibres. *Plovs One* 2011; 6: e21833.
42. Hardy JG, Pfaff A, Leal-Egaña A, et al. Glycopolymers functionalization of engineered spider silk protein-based materials for improved cell adhesion. *Macromol Biosci* 2014; 14: 936–942.
43. Wu S, Johansson J, Damdimopoulou P, et al. Spider silk for xeno-free long-term self-renewal and differentiation of human pluripotent stem cells. *Biomaterials* 2014; 35: 8496–8502.
44. Johansson J and Rising A. Evaluation of functionalized spider silk matrices: choice of cell types and controls are important

- for detecting specific effects. *Frontiers in Bioengineering and Biotechnology* 2014; 2: 50.
45. Zhu B, Li W, Lewis RV, et al. E-spun composite fibers of collagen and dragline silk protein: fiber mechanics, biocompatibility, and application in stem cell differentiation. *Biomacromolecules* 2015; 16: 202–213.
  46. Shalaly ND, Ria M, Johansson U, et al. Silk matrices promote formation of insulin-secreting islet-like clusters. *Biomaterials* 2016; 90: 50–61.
  47. Salehi S, Koeck K and Scheibel T. Spider silk for tissue engineering applications. *Molecules* 2020; 25(2): 737.
  48. Kramer JPM, Aigner TB, Petzold J, et al. Recombinant spider silk protein eADF4(C16)-RGD coatings are suitable for cardiac tissue engineering. *Scientific reports* 2020; 10: 8789.
  49. Johansson U, Widhe M, Shalaly ND, et al. Assembly of functionalized silk together with cells to obtain proliferative 3D cultures integrated in a network of ECM-like microfibers. *Scientific reports* 2019; 9: 6291.
  50. Huemmerich D, Scheibel T, Vollrath F, et al. Novel assembly properties of recombinant spider dragline silk proteins. *Curr Biol* 2004; 14: 2070–2074.
  51. Ittah S, Barak N and Gat U. A proposed model for dragline spider silk self-assembly: insights from the effect of the repetitive domain size on fiber properties. *Biopolymers* 2010; 93: 458–468.
  52. McCune J, Hawke RL, LeCluyse EL, et al. In vivo and in vitro induction of human cytochrome P4503A4 by dexamethasone. *Clinical Pharmacology & Therapeutics* 2000; 68: 356–366.
  53. Nuno Sales C, Bruno Silva L, Lara T, et al. Drug withdrawal due to safety: a review of the data supporting withdrawal decision. *Current Drug Safety* 2020; 15: 4–12.
  54. Lewicka M, Hermanson O and Rising AU. Recombinant spider silk matrices for neural stem cell cultures. *Biomaterials* 2012; 33: 7712–7717.
  55. Fredriksson C, Hedhammar M, Feinstein R, et al. Tissue response to subcutaneously implanted recombinant spider silk: an in vivo study. *Materials* 2009; 2: 1908–1922.
  56. Lee W, Choi JH, Lee S, et al. Fabrication and characterization of silk fibroin microfiber-incorporated bone marrow stem cell spheroids to promote cell-cell interaction and Osteogenesis. *ACS Omega* 2020; 5: 18021–18027.